

# Optically induced magnetization and ultrafast spin relaxation in manganese oxide

T. Kohmoto,<sup>1</sup> H. Sakaguchi,<sup>2</sup> M. Takahashi,<sup>1</sup> K. Kakita,<sup>1</sup> Y. Koyama,<sup>1</sup> and T. Moriyasu<sup>2</sup>

<sup>1</sup>Graduate School of Science, Kobe University, Nada, Kobe 657-8501, Japan

<sup>2</sup>Graduate School of Science and Technology, Kobe University, Nada, Kobe 657-8501, Japan

(Received 19 July 2008; revised manuscript received 19 September 2008; published 24 October 2008)

The optically induced magnetization and ultrafast spin relaxation in an antiferromagnet MnO were observed by polarization spectroscopy with the pump-probe technique. The spin relaxation time in the picosecond region was measured at temperatures from 6 up to 800 K. The observed spin relaxation is the sum of the spin-spin relaxation and the spin-lattice relaxation. At lower temperatures below room temperature, the temperature-independent spin-spin relaxation is dominant. A stepped decrease in the spin relaxation rate was observed near the Néel temperature  $T_N=118$  K, where the long-range order is lost. At higher temperatures above room temperature, the temperature-dependent spin-lattice relaxation is dominant. The observed spin-lattice relaxation rate has a  $T^2$  dependence instead of the  $T^9$  dependence well known in magnetic-resonance measurements for the Raman process of phonons. The observed temperature dependence can be explained by the conventional theory of spin-lattice relaxation for the Raman process by taking account of the effect of the Debye temperature of the crystal.

DOI: [10.1103/PhysRevB.78.144420](https://doi.org/10.1103/PhysRevB.78.144420)

PACS number(s): 76.30.Fc, 78.47.jc, 78.20.Ls

## I. INTRODUCTION

Ultrafast magnetization dynamics has recently become one of the most attractive topics in condensed matter physics and its understanding is strongly desired from fundamental and technological viewpoints.<sup>1-5</sup> The study on the ultrafast magnetization dynamics and optical control of magnetization has potential applications for the developments of ultrafast spin control,<sup>6-9</sup> spintronics,<sup>10-12</sup> quantum computing,<sup>13-16</sup> and optical control of correlated spin systems.<sup>17-21</sup>

Ultrashort laser pulses enable us to observe the ultrafast spin dynamics near and above room temperature in the picosecond and femtosecond regions, which could not be observed by the conventional techniques of magnetic resonance. However, the spin dynamics and spin relaxation at higher temperatures are not necessarily understood completely. In a rare-earth ion in crystals, we reported that the temperature dependence of the spin-lattice relaxation rate for the Raman process near room temperature deviates from the  $T^9$  dependence of phonons observed at low temperatures.<sup>22</sup>

In the study on the fast spin dynamics in condensed matter near room temperature, the optical pumping with short laser pulses is very useful. The observation of the spin relaxation<sup>23,24</sup> and the free-induction-decay signal<sup>25</sup> of transition-metal ions in crystals and solutions have been reported, where the optically induced magnetization was detected by pickup coils and the resolution time of the detection system was of the order of nanoseconds. If the induced magnetization can be probed by optical pulses, the time resolution can be remarkably improved and the ultrafast spin dynamics in picosecond or femtosecond region can be observed. Such studies on the ultrafast spin dynamics have been reported in semiconductors,<sup>26-28</sup> metals,<sup>29,30</sup> and strongly correlated insulators.<sup>31</sup>

The study on the spin-lattice relaxation in MnO has not been reported so far. It is because the relaxation time is in the picosecond region and the observation of the spin-lattice relaxation by the conventional magnetic-resonance technique

is not easy. In the present paper we report on the observation of optically induced magnetization and ultrafast spin relaxation in the ground state of MnO from low temperatures up to 800 K. The magnetization is created by an optical pump pulse, and spin relaxation times of the order of picoseconds or femtoseconds can be obtained from the decay curves of the magnetization. Such ultrashort relaxation times cannot be measured by the conventional electron spin resonance (ESR), whose time resolution is nanoseconds at best. The time resolution of our optical method is limited only by the temporal width of the light pulses, and investigation of ultrafast spin dynamics can be realized. In MnO, the possibility of a high-temperature short-range-order transition was discussed in the experiment of spin-polarized photoelectron diffraction.<sup>32,33</sup> The observation of optically induced magnetization is very useful for the study on the high-temperature spin dynamics.

At room temperature, MnO is a paramagnetic insulator with a cubic rock salt structure. Below the Néel temperature  $T_N=118$  K, it transforms to an antiferromagnetic phase. The transition from the paramagnetic phase to the antiferromagnetic phase at  $T_N$  is driven by nearest-neighbor and next-nearest-neighbor antiferromagnetic interactions.<sup>34</sup> The magnetic moments on Mn atoms align ferromagnetically within a (111) plane, and these planes are stacked antiferromagnetically in the direction normal to the (111) plane.<sup>35-37</sup> At temperatures below  $T_N$ , the magnetic system will break up into multiple domains corresponding to the antiferromagnetic stacking along different possible [111] directions within the crystal.

In the experiment, the pump-probe technique is used to observe the spin relaxation in the ground state of the divalent manganese ion in a MnO single crystal. The circular dichroism and the circular birefringence of the optical transition are responsible for the creation and the detection of the magnetization. The longitudinal spin relaxation time  $T_1$ , which is of the order of picoseconds, is obtained from the observed decay curve of the magnetization. The spin relaxation at higher temperatures is caused by the Raman process of phonons. In

many ESR measurements, the relaxation rate for the Raman process for the Kramers ion has the temperature dependence of  $1/T_1 \propto T^9$ . The temperature dependence of  $1/T_1$  observed in our experiment, however, shows much smaller change than that expected from the  $T^9$  dependence. We show that the observed  $T^2$  dependence of  $1/T_1$  can be explained by the conventional theory of spin-lattice relaxation for the Raman process of phonons.

## II. EXPERIMENT

The pump pulse is provided by a Ti:sapphire regenerative amplifier and the probe pulse by an optical parametric amplifier. The wavelength of the pump pulse is 790 nm. The wavelength 900 nm is used for the probe pulse to avoid the strong absorption<sup>38</sup> in the visible region and to get enough transmitted intensity. We observed the decay curves of the optically induced magnetization in the picosecond region in the temperature range from 6 up to 800 K. The sample is in a temperature-controlled refrigerator for the measurement below room temperature and in a temperature-controlled metal block in a evacuated vessel for the measurement above room temperature. The circularly polarized pump pulse and the linearly polarized probe pulse are nearly collinear and focused on the sample. The thickness of the sample is 0.1 mm, and the direction of the laser beams is perpendicular to the (111) surface of the sample. The waist size of the beams at the sample is about 100  $\mu\text{m}$ . The pulse energy and the pulse width at the sample are  $\sim 2 \mu\text{J}$  and 0.5 ps for the pump pulse and  $\sim 0.1 \mu\text{J}$  and 0.2 ps for the probe pulse. The repetition rate of the pulses is 1 kHz.

The population differences, or magnetization, in the magnetic sublevels of the ground state are instantaneously created by the circularly polarized pump pulse. The created magnetization is detected by a polarimeter as the change of the polarization of the linearly polarized probe pulse.

The polarimeter<sup>22,39</sup> detects the rotation of polarization plane of a light beam. A linearly polarized beam is split by a Glan prism and incident on two photodiodes whose photocurrents are subtracted at a resistor. When the Glan prism is mounted at an angle of  $45^\circ$  to the plane of polarization of the light beam, the two photocurrents cancel. If the plane of polarization rotates, the two currents do not cancel and the voltage appears at the resistor.

In the present experiment, the magnetization in the ground state is created by the pump pulse, and then the circular dichroism and/or the circular birefringence of the optical transition are induced in the sample. The linearly polarized probe pulse is considered to be a sum of two circularly polarized components which have the opposite polarizations and the same intensities. In the case of the circular dichroism, the induced circular dichroism creates an amplitude difference between the two circularly polarized components of the transmitted probe pulse. The two circularly polarized components are transformed by a quarter-wave plate to two linearly polarized components whose polarizations crossed each other, and the amplitude difference between the two circularly polarized components is transformed to an amplitude difference between the two linearly polarized compo-

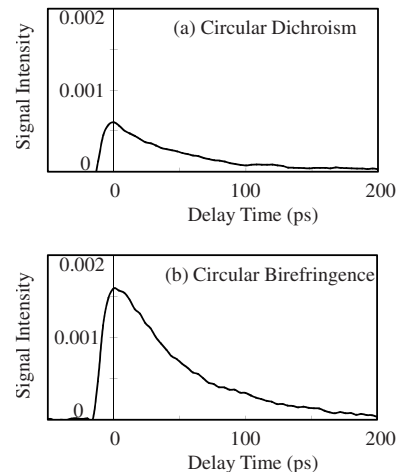


FIG. 1. Observed decay curves of the magnetization in MnO at room temperature detected (a) by the circular dichroism and (b) by the circular birefringence.

nents or a rotation of polarization plane. This rotation is detected by the polarimeter as the signal of magnetization. In the case of the circular birefringence, on the other hand, the induced circular birefringence creates a phase difference between the two circularly polarized components of the transmitted probe pulse. This phase difference results in a rotation of polarization plane, and this rotation is detected directly by the polarimeter without the quarter-wave plate as the signal of magnetization. Thus, the circular dichroism and the circular birefringence can be detected separately by the polarimeter with and without a quarter-wave plate.

The time evolution of the magnetization is observed by changing the optical delay between the pump and probe pulses. The longitudinal spin relaxation time  $T_1$  is obtained from the decay curve of the magnetization. In order to improve the signal-to-noise ratio, the sign of the circular polarization of the pump pulse is switched shot by shot by using a photoelastic modulator, and the output signal from the polarimeter is lock-in detected.

## III. EXPERIMENTAL RESULTS

The observed decay curves of the magnetization in MnO at room temperature are shown in Fig. 1. Figures 1(a) and 1(b) show the magnetization signal detected by the circular dichroism and the circular birefringence, respectively. The vertical axis in Fig. 1(a) corresponds to ellipticity of the circular polarization and that in Fig. 1(b) corresponds to Faraday rotation angle in radian. As in seen in Fig. 1, the signal detected by the circular birefringence is larger than that by the circular dichroism in our experimental condition. The detection by the circular birefringence corresponds to that of time-resolved Faraday rotation.<sup>3</sup>

The temperature dependence of the decay curve of the magnetization in MnO detected by the circular birefringence is shown in Fig. 2, where the vertical axis is Faraday rotation angle. The obtained longitudinal relaxation times are 58, 102, 88, and 50 ps for 6, 120, 440, and 740 K, respectively. The relaxation time at low temperatures is  $\sim 60$  ps. Near the

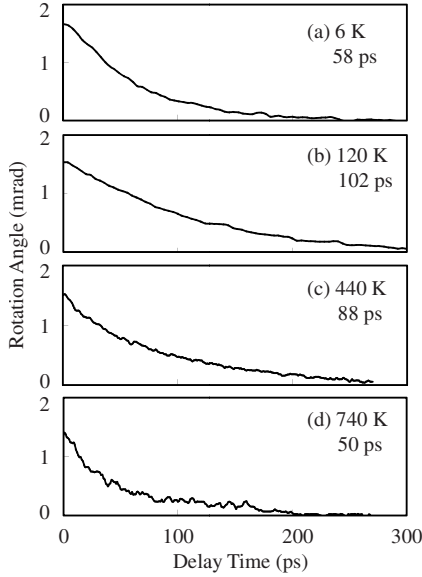


FIG. 2. Temperature dependence of the decay curve of the magnetization in MnO detected by the circular birefringence. The vertical axis is Faraday rotation angle.

Néel temperature, it increases abruptly to  $\sim 100$  ps, and then decreases gradually as the temperature is increased.

The temperature dependence of the longitudinal relaxation rate  $1/T_1$  in MnO obtained from the observed decay curve of the magnetization is shown in Fig. 3. Figure 4 shows that at lower temperatures. The spin relaxation rate at low temperatures is nearly constant up to 80 K. A stepped decrease in the relaxation rate appears near the Néel temperature. Then, above 120 K, it increases gradually and monotonously as the temperature is increased. In our experiment, the spin relaxation in the picosecond region can be observed in the very wide range of temperature between 6 and 800 K by using the ultrafast polarization spectroscopy. However, there is no order change in the spin relaxation rate, and the ratio of the maximum and minimum values of the relaxation rate is less than three in the whole temperature region. This is considered to be because the temperature-independent spin-spin relaxation dominates at lower temperatures.

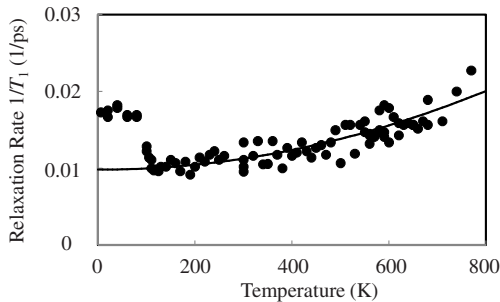


FIG. 3. Temperature dependence of the longitudinal relaxation rate  $1/T_1$  in MnO obtained from the observed decay curve of the magnetization. The solid curve presents a best fit of Eq. (4) to the observed data of  $1/T_1$  above 120 K.

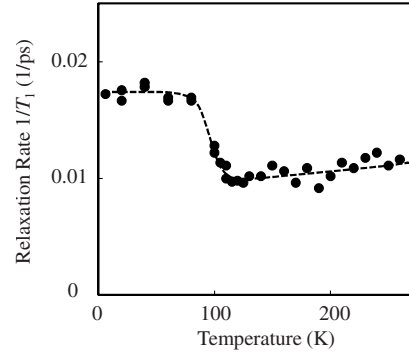


FIG. 4. Temperature dependence of the longitudinal relaxation rate  $1/T_1$  in MnO at lower temperatures. The broken curve serves as a visual guide.

#### IV. DISCUSSION

The spin-lattice relaxation at higher temperatures is explained by the Raman process of phonons. In the Raman process, the population distribution in the magnetic sublevels of the ground state is changed through a process caused by a phonon pair. One phonon is absorbed and induces the transition from one of the ground state to a virtual state, and at the same time the other phonon is emitted and induces another transition from the virtual state to the other of the ground state. Any two phonons can take part if their frequency difference is equal to the resonance frequency of the magnetic system, and then the Raman process becomes dominant at higher temperatures where many thermal phonons exist. The observed spin relaxation at higher temperatures is considered to be caused by the Raman process of phonons. In many materials studied by ESR at low temperatures, the spin-lattice relaxation rate due to the Raman process for the Kramers ion shows the temperature dependence  $1/T_1 = CT^9$ . The temperature dependence of  $1/T_1$  in Fig. 3 obtained in our experiment at higher temperatures, however, has much smaller change than that expected from the  $T^9$  dependence. The observed spin relaxation rate is considered to be a sum of the temperature-independent spin-spin relaxation and the temperature-dependent spin-lattice relaxation. The latter seems to have a  $T^2$  dependence rather than the  $T^9$  dependence at higher temperatures.

Here, in order to explain this experimental results, we consider the Debye model of lattice vibration. Turning back to the beginning of the theory of the Raman process, the expression of the relaxation rate due to the Raman process for the Kramers ion is presented by<sup>40</sup>

$$\begin{aligned} \frac{1}{T_1} &= K \int_0^{\omega_m} \frac{\omega^8 \exp(\hbar\omega/kT)}{\{\exp(\hbar\omega/kT) - 1\}^2} d\omega \\ &= K \left( \frac{kT}{\hbar} \right)^9 \int_0^{\theta_D/T} \frac{x^8 e^x}{(e^x - 1)^2} dx, \end{aligned} \quad (1)$$

where  $K$  is a constant determined by the interaction between the magnetic ions and the lattice vibrations,  $\omega$  is the phonon frequency, and  $\omega_m$  is the maximum phonon frequency corresponding to the Debye temperature  $\theta_D$  ( $\hbar\omega_m = k\theta_D$ ). Equation

(1) means that the Raman process is caused by the phonons with frequencies below  $\omega_m$ . In the case of low temperatures ( $T \ll \theta_D$ ), the upper limit  $\theta_D/T$  of the integral in Eq. (1) can be regarded as infinity, and the integral becomes a constant. Then the well-known  $T^9$  dependence is derived from Eq. (1). In most of the conventional ESR studies on the relaxation,  $T \ll \theta_D$  is a good approximation and the  $T^9$  dependence is valid for the relaxation analysis.

In the case of higher temperatures ( $T \geq \theta_D$ ), the integral in Eq. (1) can no longer be regarded as a constant but depends on the temperature. In such a case, as in the case of our experiment, we have to consider the relaxation rate in Eq. (1) taking account of the temperature-dependent integral. Equation (1) can be rewritten as

$$\frac{1}{T_1} = CT^9 f\left(\frac{T}{\theta_D}\right),$$

$$f\left(\frac{T}{\theta_D}\right) = \frac{1}{8!} \int_0^{\theta_D/T} \frac{x^8 e^x}{(e^x - 1)^2} dx. \quad (2)$$

When  $\theta_D/T \rightarrow \infty$ , the integral approaches  $8!$  and  $f(T/\theta_D) \rightarrow 1$ . Then Eq. (2) becomes  $1/T_1 = CT^9$ . When  $\theta_D/T \rightarrow 0$ , on the other hand, the integrand approximates to  $x^6$  ( $x \ll 0$ ) and the spin-lattice relaxation rate is expected as  $1/T_1 \propto T^2$ .

$$\frac{1}{T_1} \propto \begin{cases} T^9 & (T \ll \theta_D) \\ T^2 & (T \gg \theta_D). \end{cases} \quad (3)$$

The Debye temperature for MnO is known as  $\theta_D = 230$  K.<sup>41</sup>

The solid curve in Fig. 3 presents a best fit to the observed data of  $1/T_1$  above 120 K, where the fitting function is

$$\frac{1}{T_1} = A + CT^9 f\left(\frac{T}{\theta_D}\right). \quad (4)$$

The fitting parameters are  $A = (9.8 \pm 1.0) \times 10^9 \text{ s}^{-1}$  and  $C = (1.3 \pm 0.2) \times 10^{-7} \text{ s}^{-1} \text{ K}^{-9}$ . The constant term represents the spin-spin relaxation and the second term represents the spin-lattice relaxation. Figure 5 shows the log-log plot of the temperature dependence of the spin relaxation rate in Fig. 3. The solid circles are the observed spin relaxation rate. In order to clarify the contributions from each term, the constant spin-spin term  $A$  and the Raman-process term  $CT^9 f(T/\theta_D)$  are also shown separately by the dotted line and the broken curve, respectively, in Fig. 5. As is seen, the spin relaxation in MnO below room temperature is dominated by the temperature-independent spin-spin relaxation. The spin-lattice relaxation becomes dominant above room temperature where the Raman process of phonons shows the  $T^2$  dependence instead of the  $T^9$  dependence. Our experimental results are explained well by the sum of the spin-spin relaxation and the Raman process of phonons in Eq. (4). The  $T^2$  dependence at higher temperatures is caused by the lack of high frequency phonons in the Raman process; the distribution of the phonon frequency has the upper limit corresponding to the Debye temperature.

In the previous work on a rare-earth ion doped in crystals,<sup>22</sup> we reported that the temperature dependence of the spin-lattice relaxation rate for the Raman process has a  $T^9$

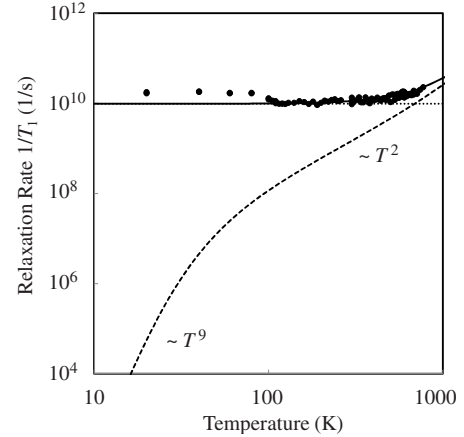


FIG. 5. Log-log plot of the temperature dependence of the spin relaxation rate  $1/T_1$  in Fig. 3. The solid circles are the observed spin relaxation rate and the solid curve presents a best fit of Eq. (4) to the observed data of  $1/T_1$  above 120 K. The contributions from the constant spin-spin term  $A$  and the Raman-process term  $CT^9 f(T/\theta_D)$  are also shown separately by the dotted line and the broken curve, respectively.

dependence in low temperatures but deviates from that near room temperature. In dilute spin systems such as the previous case, the contribution of the spin-spin relaxation is negligible even at low temperatures and the contribution of the Raman process of phonons dominates in a wide temperature range. In dense spin systems such as the present case, however, the distance between magnetic ions is short and the temperature-independent spin-spin relaxation dominates up to room temperature. The contribution of the Raman process appears above room temperature where the spin-spin relaxation rate is proportional to  $T^2$ .

The spin-spin relaxation is caused by the magnetic interaction between the manganese ions, which contains the magnetic dipole interaction and the exchange interaction. At low temperatures below the antiferromagnetic phase transition point, the magnetic long-range order among the manganese spins builds up. The spins reversed by the optical pulse are brought back to the ordered state through the magnetic interaction. The long-range order accelerates the bringing back and increases the spin relaxation rate. Above the Néel temperature, the long-range order is lost and the acceleration is reduced. This results in the stepped decrease in the spin relaxation rate near the Néel temperature.

Another possibility for the decay of probed magnetization is magnetization transport from the excited spot due to the spin diffusion. To examine this possibility, we tried to observe the transported magnetization created by a separated pump beam from the probe beam. However, no magnetization signal was observed for the separation of  $\sim 100 \mu\text{m}$ . The spin diffusion has small contribution to the magnetization decay in MnO.

In classical simple spin systems, spin-spin interactions are considered to conserve the total magnetization and the decay of magnetization is not expected. In quantum spin systems in solids, on the other hand, the decay of magnetization occurs, where the dephasing time is very short and the dephasing process or decay of off-diagonal density-matrix elements be-



tween up and down spin states plays an important role.<sup>42</sup> The theoretical investigation of spin-spin relaxation, or spin cross relaxation, was initiated by Bloembergen *et al.*<sup>43</sup> and Grant.<sup>44,45</sup> In a theory of the cross relaxation for randomly distributed dilute spin systems, the decay curve of  $\exp(-\sqrt{\Gamma}t)$  is predicted.<sup>42</sup> However, there is no appropriate theory of spin-spin relaxation that gives the relaxation time directly corresponding to the present case.

Here we estimate the lower limit of the relaxation time of magnetization in MnO using the second-moment method, which is used to calculate the spectral broadening due to the spin-spin interaction in magnetic resonance.<sup>46</sup> The second moment  $\langle(\Delta\nu)^2\rangle$  for the magnetic dipole-dipole interaction for like spins is given by<sup>47</sup>

$$\langle(\Delta\nu)^2\rangle = \frac{3}{5} \frac{g^4 \mu_B^4}{h^2} S(S+1) \sum_k \frac{1}{r_{jk}^6}, \quad (5)$$

where  $g$ ,  $\mu_B$ , and  $S$  are the  $g$  factor, Bohr magneton, and spin angular momentum, respectively. The distance  $r_{jk}$  between manganese ions can be obtained from the cubic rock salt structure and its lattice constant  $a=0.443$  nm. Substituting  $S=5/2$  and  $g=2$  and taking account of the nearest-neighbor and next-nearest-neighbor ions, the inhomogeneous frequency broadening calculated from Eq. (5) is given by  $\Delta\nu \sim 14$  GHz. Assuming a Gaussian line shape, the lower limit of the relaxation time  $T_d$  for the magnetic dipole-dipole interaction is obtained as

$$T_d = \frac{\sqrt{2}}{2\pi\Delta\nu} \frac{1}{\Delta\nu} \sim 16 \text{ ps}. \quad (6)$$

In MnO the exchange interaction has to be taken into account. Next we estimate the lower limit of the spin-spin relaxation time in MnO using the uncertainty principle  $\Delta E \Delta t \geq \hbar$ . If we consider the exchange energy  $J \sim 15$  K (Ref. 34) as the uncertainty  $\Delta E$  of energy, the uncertainty of time becomes  $\Delta t \geq \hbar/\Delta E \sim 0.5$  ps. This tells us that the spin-spin relaxation time is longer than 0.5 ps. These estimations above are not inconsistent with the observed spin-spin relaxation time  $\sim 60$  ps at low temperatures, but do not present the spin-spin relaxation time itself.

In the experiment of spin-polarized photoelectron diffraction, an abrupt change in the temperature dependence of x-ray photoelectron spectrum was observed in  $\text{KMnF}_3$  (Ref. 48) and MnO (Ref. 32) and a high-temperature short-range-order transition was discussed. In MnO, it was suggested that a short-range-order transition occurs at  $\sim 530$  K.<sup>33</sup> In the present experiment, however, no anomalous change in the spin relaxation rate was observed around the corresponding temperature, while its large change was observed near the long-range-order transition temperature  $T_N$ . The transmitted probe pulses are used in the present experiment, and the information on bulk spins is provided. In the experiment of spin-polarized photoelectron diffraction, on the other hand, the information on spins in a few layers from the surface is provided. Our experimental result supports the Monte Carlo study on simple-cubic Ising lattices,<sup>49</sup> where the observed abrupt change in the photoelectron spectrum was suggested to be due to a surface-specific magnetic transition.

## V. SUMMARY

We observed the optically induced magnetization and the ultrafast spin relaxation in an antiferromagnet MnO by using pump-probe polarization spectroscopy. The spin relaxation time in the picosecond region in the wide temperature range from 6 up to 800 K was measured by the optical method. The observed spin relaxation is the sum of the spin-spin relaxation and the spin-lattice relaxation. At lower temperatures below room temperature, the temperature-independent spin-spin relaxation is dominant. A stepped decrease in the spin relaxation rate was observed near the Néel temperature where the long-range order is lost. At higher temperatures above room temperature, the temperature-dependent spin-lattice relaxation is dominant. The observed values of the spin-lattice relaxation rate at higher temperatures cannot be explained by the well-known  $T^9$  dependence for the Raman process of phonons. We considered the Debye model of lattice vibration, and the observed  $T^2$  dependence is explained by taking account of the effect of the Debye temperature of the crystal. No anomalous change in the spin relaxation rate was observed around the temperature where the abrupt decrease of short range order was suggested in the experiment of spin-polarized photoelectron diffraction.

<sup>1</sup>I. Tudosa, C. Stamm, A. B. Kashuba, F. King, H. C. Siegmann, J. Stöhr, G. Ju, B. Lu, and D. Weller, *Nature (London)* **428**, 831 (2004).

<sup>2</sup>A. V. Kimel, A. Kirilyuk, P. A. Usachev, R. V. Pisarev, A. M. Balbashov, and Th. Rasing, *Nature (London)* **435**, 655 (2005).

<sup>3</sup>S. A. Wolf, D. D. Awschalom, R. A. Buhrman, J. M. Daughton, S. von Molnár, M. L. Roukes, A. Y. Chtchelkanova, and D. M. Treger, *Science* **294**, 1488 (2001).

<sup>4</sup>R. C. Myers, M. H. Mikkelsen, J.-M. Tang, A. C. Gossard, M. E. Flatté, and D. D. Awschalom, *Nature Mater.* **7**, 203 (2008).

<sup>5</sup>D. D. Awschalom, N. Samarth, and D. Loss, *Semiconductor Spintronics and Quantum Computation* (Springer-Verlag, Berlin, 2002).

<sup>6</sup>A. V. Kimel, A. Kirilyuk, A. Tsvetkov, R. V. Pisarev, and Th. Rasing, *Nature (London)* **429**, 850 (2004).

<sup>7</sup>R. Gómez-Abal, O. Ney, K. Satitkovitchai, and W. Hübner, *Phys. Rev. Lett.* **92**, 227402 (2004).

<sup>8</sup>C. Stamm, I. Tudosa, H. C. Siegmann, J. Stöhr, A. Yu. Dobin, G. Woltersdorf, B. Heinrich, and A. Vaterlaus, *Phys. Rev. Lett.* **94**, 197603 (2005).

<sup>9</sup>C. D. Stanciu, F. Hansteen, A. V. Kimel, A. Kirilyuk, A. Tsukamoto, A. Itoh, and Th. Rasing, *Phys. Rev. Lett.* **99**, 047601 (2007).

<sup>10</sup>A. Greilich, R. Oulton, E. A. Zhukov, I. A. Yugova, D. R. Yakovlev, M. Bayer, A. Shabaev, Al. L. Efros, I. A. Merkulov, V. Stavarache, D. Reuter, and A. Wieck, *Phys. Rev. Lett.* **96**,

- 227401 (2006).
- <sup>11</sup>Y. Wu, E. D. Kim, X. Xu, J. Cheng, D. G. Steel, A. S. Bracker, D. Gammon, S. E. Economou, and L. J. Sham, *Phys. Rev. Lett.* **99**, 097402 (2007).
  - <sup>12</sup>Y. Li, Y. Chye, Y. F. Chiang, K. Pi, W. H. Wang, J. M. Stephens, S. Mack, D. D. Awschalom, and R. K. Kawakami, *Phys. Rev. Lett.* **100**, 237205 (2008).
  - <sup>13</sup>R.-B. Liu, W. Yao, and L. J. Sham, *Phys. Rev. B* **72**, 081306(R) (2005).
  - <sup>14</sup>Y. Wu, X. Li, L. M. Duan, D. G. Steel, and D. Gammon, *Phys. Rev. Lett.* **96**, 087402 (2006).
  - <sup>15</sup>R. S. Kolodka, A. J. Ramsay, J. Skiba-Szymanska, P. W. Fry, H. Y. Liu, A. M. Fox, and M. S. Skolnick, *Phys. Rev. B* **75**, 193306 (2007).
  - <sup>16</sup>S. M. Clark, Kai-Mei C. Fu, T. D. Ladd, and Y. Yamamoto, *Phys. Rev. Lett.* **99**, 040501 (2007).
  - <sup>17</sup>N. P. Duong, T. Satoh, and M. Fiebig, *Phys. Rev. Lett.* **93**, 117402 (2004).
  - <sup>18</sup>F. Hansteen, A. Kimel, A. Kirilyuk, and T. Rasing, *Phys. Rev. Lett.* **95**, 047402 (2005).
  - <sup>19</sup>S. Tomimoto, M. Matsubara, T. Ogasawara, H. Okamoto, T. Kimura, and Y. Tokura, *Phys. Rev. Lett.* **98**, 017402 (2007).
  - <sup>20</sup>J. Wang, I. Cotoros, K. M. Dani, X. Liu, J. K. Furdyna, and D. S. Chemla, *Phys. Rev. Lett.* **98**, 217401 (2007).
  - <sup>21</sup>M. Matsubara, Y. Okimoto, T. Ogasawara, Y. Tomioka, H. Okamoto, and Y. Tokura, *Phys. Rev. Lett.* **99**, 207401 (2007).
  - <sup>22</sup>T. Kohmoto, Y. Fukuda, M. Kunitomo, and K. Isoda, *Phys. Rev. B* **62**, 579 (2000).
  - <sup>23</sup>J. P. van der Ziel and N. Bloembergen, *Phys. Rev.* **138**, A1287 (1965).
  - <sup>24</sup>Y. Takagi, *Opt. Commun.* **59**, 122 (1986).
  - <sup>25</sup>Y. Takagi, Y. Fukuda, and T. Hashi, *Opt. Commun.* **55**, 115 (1985).
  - <sup>26</sup>A. V. Kimel, V. V. Pavlov, R. V. Pisarev, V. N. Gridnev, F. Bentivegna, and Th. Rasing, *Phys. Rev. B* **62**, R10610 (2000).
  - <sup>27</sup>A. V. Kimel, F. Bentivegna, V. N. Gridnev, V. V. Pavlov, R. V. Pisarev, and Th. Rasing, *Phys. Rev. B* **63**, 235201 (2001).
  - <sup>28</sup>J. Wang, L. Cywiński, C. Sun, J. Kono, H. Muneke, and L. J. Sham, *Phys. Rev. B* **77**, 235308 (2008).
  - <sup>29</sup>B. Koopmans, M. van Kampen, J. T. Kohlhepp, and W. J. M. de Jonge, *Phys. Rev. Lett.* **85**, 844 (2000).
  - <sup>30</sup>D. Cheskis, A. Porat, L. Szapiro, O. Potashnik, and S. Bar-Ad, *Phys. Rev. B* **72**, 014437 (2005).
  - <sup>31</sup>V. V. Pavlov, R. V. Pisarev, V. N. Gridnev, E. A. Zhukov, D. R. Yakovlev, and M. Bayer, *Phys. Rev. Lett.* **98**, 047403 (2007).
  - <sup>32</sup>B. Hermsmeier, J. Osterwalder, D. J. Friedman, and C. S. Fadley, *Phys. Rev. Lett.* **62**, 478 (1989).
  - <sup>33</sup>B. Hermsmeier, J. Osterwalder, D. J. Friedman, B. Sinkovic, T. Tran, and C. S. Fadley, *Phys. Rev. B* **42**, 11895 (1990).
  - <sup>34</sup>J. E. Pask, D. J. Singh, I. I. Mazin, C. S. Hellberg, and J. Kortus, *Phys. Rev. B* **64**, 024403 (2001).
  - <sup>35</sup>W. L. Roth, *Phys. Rev.* **110**, 1333 (1958).
  - <sup>36</sup>B. F. Woodfield, J. L. Shapiro, R. Stevens, J. Boerio-Goates, and M. L. Wilson, *Phys. Rev. B* **60**, 7335 (1999), and references therein.
  - <sup>37</sup>A. L. Goodwin, M. G. Tucker, M. T. Dove, and D. A. Keen, *Phys. Rev. Lett.* **96**, 047209 (2006).
  - <sup>38</sup>D. R. Huffman, R. L. Wild, and M. Shinmei, *J. Chem. Phys.* **50**, 4092 (1969).
  - <sup>39</sup>R. V. Jones, *Proc. R. Soc. London, Ser. A* **349**, 423 (1976).
  - <sup>40</sup>A. Abragam and B. Bleaney, *Electron Paramagnetic Resonance of Transition Ions* (Clarendon, Oxford, 1970), Chap. 10.
  - <sup>41</sup>R. E. Nettleton, *Phys. Rev.* **135**, A1023 (1964).
  - <sup>42</sup>T. Endo and T. Muramoto, *Phys. Rev. B* **29**, 6043 (1984).
  - <sup>43</sup>N. Bloembergen, S. Shapiro, P. S. Pershan, and J. O. Artman, *Phys. Rev.* **114**, 445 (1959).
  - <sup>44</sup>W. J. C. Grant, *Phys. Rev.* **134**, A1554 (1964).
  - <sup>45</sup>W. J. C. Grant, *Phys. Rev.* **134**, A1565 (1964).
  - <sup>46</sup>A. Abragam, *The Principle of Nuclear Magnetism* (Clarendon, Oxford, 1961).
  - <sup>47</sup>J. H. Van Vleck, *Phys. Rev.* **74**, 1168 (1948).
  - <sup>48</sup>B. Sinković, B. Hermsmeier, and C. S. Fadley, *Phys. Rev. Lett.* **55**, 1227 (1985).
  - <sup>49</sup>F. Zhang, S. Thevuthasan, R. T. Scalettar, R. R. P. Singh, and C. S. Fadley, *Phys. Rev. B* **51**, 12468 (1995).